

ON THE ATOMIC STATES OF Σ^- HYPERONS AND THE ΣN INTERACTION

JANUSZ DĄBROWSKI AND JACEK ROŻYNEK

Theoretical Division, A. Sołtan Institute for Nuclear Studies
Hoża 69, 00-681 Warsaw, Poland

(Received May 14, 2002)

The Nijmegen baryon–baryon interaction models are used to determine the Σ^- single particle potential in nuclei. For the ΣA conversion cross section — which appears in the expression for the imaginary part of the Σ^- potential — two alternative parametrizations are used. With the help of this complex Σ^- potential the energy shifts and widths of the observed levels of Σ^- atoms are calculated. Comparison with the 23 existing data shows that the lowest χ^2 is obtained with the Nijmegen model F which leads to the Σ^- potential which is repulsive inside nuclei and has an attractive pocket at the nuclear surface. The reasonable accuracy of the perturbation approximation is discussed. The sensitivity of the results to the tail of the nucleon density distributions is investigated.

PACS numbers: 13.75.Ev, 36.10.Gv

1. Introduction

The available data on strong interaction effects in Σ^- atoms, shown in Table I, consist of 23 data points: strong-interaction shifts ε and widths Γ of the observed levels. These shifts and widths can be measured directly only in the lowest Σ^- atomic levels with the principle quantum number n and with the orbital quantum number $l = n - 1$ (in the observed states the orbits are circular). The widths of the $n + 1$ ‘upper’ levels can be obtained indirectly from measurements of the relative yields of X-rays. As seen in Table I the accuracy of the data is limited. Nevertheless these data provide us with valuable information on the interaction between Σ^- and nucleons.

This information was used in [4] and [5] (hereafter referred to as I and II) to determine the best among the Nijmegen models of the baryon–baryon interaction [6–9], *i.e.*, the one which leads to the best description of the

TABLE I

Experimental values of the energy shifts ε_{exp} and widths Γ_{exp} for the lower level and the widths Γ_{exp}^u for the upper level of the indicated Σ^- atoms. All energies are in eV.

Nucl.	$n+1 \rightarrow n$	ε_{exp}	Γ_{exp}	Γ_{exp}^u
^{12}C	$4 \rightarrow 3$	—	—	$0.031 \pm 0.012^{\text{a}}$
^{16}O	$4 \rightarrow 3$	$320 \pm 230^{\text{b}}$	—	$1.0 \pm 0.7^{\text{b}}$
^{24}Mg	$5 \rightarrow 4$	$25 \pm 40^{\text{b}}$	$< 70^{\text{b}}$	$0.11 \pm 0.09^{\text{b}}$
^{27}Al	$5 \rightarrow 4$	$68 \pm 28^{\text{b}}$	$43 \pm 75^{\text{b}}$	$0.24 \pm 0.06^{\text{b}}$
^{28}Si	$5 \rightarrow 4$	$159 \pm 36^{\text{b}}$	$220 \pm 110^{\text{b}}$	$0.41 \pm 0.10^{\text{b}}$
^{32}S	$5 \rightarrow 4$	$360 \pm 220^{\text{b}}$	$870 \pm 700^{\text{b}}$	$1.5 \pm 0.8^{\text{b}}$
^{40}Ca	$6 \rightarrow 5$	—	—	$0.41 \pm 0.22^{\text{a}}$
^{48}Ti	$6 \rightarrow 5$	—	—	$0.65 \pm 0.42^{\text{a}}$
^{138}Ba	$9 \rightarrow 8$	—	—	$2.9 \pm 3.5^{\text{a}}$
^{184}W	$10 \rightarrow 9$	$214 \pm 60^{\text{c}}$	$18 \pm 149^{\text{c}}$	$2 \pm 2^{\text{c}}$
^{208}Pb	$10 \rightarrow 9$	$422 \pm 56^{\text{c}}$	$430 \pm 160^{\text{c}}$	$17 \pm 3^{\text{c}}$

^a Data taken from Ref. [1].

^b Data taken from Ref. [2].

^c Data taken from Ref. [3].

observed properties of Σ^- atoms. To determine ε and Γ , we were solving in II the Schrödinger equation, which describes the motion of Σ^- in the Σ^- atom:

$$\left[-\frac{\hbar^2}{2\mu_{\Sigma A}} \Delta + V_C(r) + \mathcal{V}(r) \right] \Psi = \mathcal{E} \Psi, \quad (1)$$

where $\mu_{\Sigma A} = M_{\Sigma} M_A / (M_{\Sigma} + M_A)$ is the Σ^- -nucleus (of mass M_A) reduced mass (M_{Σ} is the mass of Σ^-), and V_C is the Coulomb interaction between Σ^- and the nucleus.

Because of the ΣA conversion process $\Sigma^- p \rightarrow \Lambda n$, the strong interaction single particle (s.p.) potential of the Σ^- hyperon \mathcal{V} is complex, $\mathcal{V} = V + iW$, and consequently the eigenvalue \mathcal{E} is also complex, with its imaginary part connected with the width of the level, $\mathcal{E} = E - i\Gamma/2$. For the strong interaction energy shift ε , we have $\varepsilon = E_C - E$, where E_C is the pure Coulomb energy, *i.e.*, the eigenvalue of equation (1) without the strong interaction potential \mathcal{V} .

The complex potential \mathcal{V} was calculated in I and II with the help of the Nijmegen interactions in the local density approximation: the Σ^- atom was treated at each point as Σ^- moving in nuclear matter with the local proton and neutron densities $\rho_p(r)$ and $\rho_n(r)$ of the Σ^- atom,

$$\mathcal{V}(r) = \mathcal{V}_{\text{NM}}(\bar{k}_{\Sigma}, \rho_p(r), \rho_n(r)), \quad (2)$$

where \mathcal{V}_{NM} is the s.p. potential of Σ^- moving with a properly defined average momentum \bar{k}_Σ in nuclear matter with the indicated local proton and neutron densities.

The present paper is a continuation of I and II. In particular, we want to consider the following points:

- The ΣA conversion cross section σ — which appears explicitly in the procedure of calculating ε and Γ applied in I and II — is not well known. In the present paper, the results of II are extended to include two alternative parametrizations of σ .
- First order perturbation approximation was used in I, and we want to discuss the accuracy of this approximation.
- Results obtained for ε and Γ depend on the nucleon densities applied in the calculations, and we want to discuss this dependence.

2. The potential \mathcal{V}_{NM}

To calculate \mathcal{V}_{NM} , we apply the Low Order Brueckner (LOB) approximation:

$$\mathcal{V}_{\text{NM}}(k_\Sigma) = \sum_{\mathbf{k}_N} \langle \mathbf{k}_\Sigma \mathbf{k}_N | \mathcal{K} | \mathbf{k}_\Sigma \mathbf{k}_N \rangle, \tag{3}$$

where the sum runs over all occupied nucleon states with momenta \mathbf{k}_N . Spins and isospins are suppressed in our notation. \mathcal{K} denotes the ΣN Brueckner reaction matrix. In the case of the Nijmegen baryon–baryon interaction models, the reaction matrix \mathcal{K} was calculated in the LOB approximation in [9,10]. Its configuration space representation, the so called YNG interaction, was used in I and II in calculating $V_{\text{NM}} = \text{Re}\{\mathcal{V}_{\text{NM}}\}$.

To get the expression for $W_{\text{NM}} = \text{Im}\{\mathcal{V}_{\text{NM}}\}$, we replace \mathcal{K} in Eq. (3) by its imaginary part $\text{Im}\{\mathcal{K}\}$ and apply to it the optical theorem. In this way — as shown in [11,12] — we get:

$$W_{\text{NM}}(k_\Sigma, \rho_p, \rho_n) = -\frac{\hbar^2}{2\mu_{\Sigma N}} \nu' \left[\rho_p \langle k_{\Sigma p} Q \sigma \rangle + \rho_p \langle k_{\Sigma p} Q \sigma_{\Sigma p}^{\text{el}} \rangle + \rho_n \langle k_{\Sigma n} Q \sigma_{\Sigma n}^{\text{el}} \rangle \right], \tag{4}$$

where $\langle \rangle$ denotes the average value in the Fermi sea, $k_{\Sigma N}$ is the ΣN relative momentum, $\mu_{\Sigma N}$ is the ΣN reduced mass, and ν' is the ratio of the effective to the real nucleon mass. The total cross section for the elastic $\Sigma^- N$ scattering is denoted by $\sigma_{\Sigma N}^{\text{el}}$ (for $N = p$ it also includes the cross section for $\Sigma^- p \rightarrow \Sigma^0 n$). The Q operators take care that the nucleons in the final states of the respective ΣA conversion or elastic scattering processes obey the exclusion principle.

The optical theorem leads to expression (4) with the cross sections for the respective processes in nuclear matter, and we approximate these cross sections by the cross sections in free space. This approximation is particularly accurate at low densities of nuclear matter relevant for Σ^- atoms.

Now — as in I and II — we disregard the two last terms in expression (4), which contain the cross sections for the elastic Σ^-N scattering, and obtain our final expression for W_{NM} :

$$W_{\text{NM}}(k_{\Sigma}, \rho_p, \rho_n) = -\frac{\hbar^2}{2\mu_{\Sigma N}} \nu' \rho_p \langle k_{\Sigma p} Q \sigma \rangle. \quad (5)$$

This procedure, discussed in [12], ensures that the width of the Σ^- atomic states is due only to the ΣA coupling to the continuum.

For the total ΣA conversion cross section σ we use two parametrizations described in I. The first one, adjusted by Gal, Toker, and Alexander [13] to the Σ^- low energy regime up to 300 MeV/c in the laboratory frame, has the form

$$\frac{v}{c} \sigma = \left(1 + 13 \frac{v}{c}\right)^{-1} 5.1 \text{ fm}^2, \quad (6)$$

where v is the Σ^-p relative velocity.

The second one, suggested by Oset *et al.* [14] and adjusted to the Σ^- low energy regime up to 160 MeV/c, has the form:

$$\frac{v}{c} \sigma \simeq 1.7 \text{ fm}^2. \quad (7)$$

This form follows from the assumption that the transition matrix for the $\Sigma^-p \rightarrow \Lambda n$ process is constant, and only the phase space factor introduces the energy dependence of σ . The effect of this factor on $(v/c)\sigma$ is negligible in the low energy range relevant in Σ^- atoms and is not indicated in Eq. (7).

3. Results and discussion

We have followed the procedure applied in II to obtain our present results for the four models of the Nijmegen baryon–baryon interaction: models D [6], F [7], Soft-Core (SC) model [8], and the New Soft-Core (NSC) model [9].

For the average momentum \bar{k} in Eq. (2), we used zero while calculating $V(r)$, and the average value obtained with the hydrogen-like Σ^- wave function while calculating $W(r)$.

The proton and neutron density distributions were taken from the Isomorphous Shell Model (ISM) of Anagnostatos [15–18]¹.

¹ In case of ^{184}W and ^{208}Pb we assumed for the neutron density the form $\rho_n(r) = (N/Z)\rho_p(r)$.

For the Coulomb potential V_C , we use the uniform charge distribution with radius $R = \sqrt{3/5}\langle r^2 \rangle^{1/2}$ with empirical values of the mean square radius $\langle r^2 \rangle^{1/2}$ of the charge distribution (collected in [18]).

In calculating the Q operator in Eq. (5), we followed the Appendix of II.

First let us consider the Σ^- Pb atom for which we have the most precise data of Powers *at al.* [3]. Our results obtained for this case, together with values of χ^2 (Pb) calculated for the 3 experimental Pb data points, are shown in Table II. The big values of χ^2 (Pb) for models D and NSC clearly indicate that these models are completely inconsistent with the Σ^- atomic data. Consequently, we continue our discussion only for models F and SC.

TABLE II

Energy shifts ε , ε^u and widths Γ , Γ^u calculated with the indicated models of the ΣN interaction, respectively for the lower and upper level of the Σ^- Pb atom and the corresponding values of χ^2 for the 3 experimental Pb data (see Table I). All energies are in eV.

Model	ε^a	ε^b	Γ^a	Γ^b	$\varepsilon^{u a}$	$\varepsilon^{u b}$	$\Gamma^{u a}$	$\Gamma^{u b}$	χ^2 (Pb) ^a	χ^2 (Pb) ^b
D	995.4	1023.57	1250.9	995.3	29.7	30.1	29.0	20.8	148.0	129.9
F	457.4	469.1	773.4	582.1	18.9	19.2	23.8	16.7	10.3	1.7
SC	380.0	396.0	877.4	672.3	12.6	12.9	24.7	17.3	15.2	2.6
NSC	1899.5	1974.9	2603.8	2254.8	49.3	49.9	37.7	28.2	933.2	903.6

^a Expression (6) was applied for σ .

^b Expression (7) was applied for σ .

Table III contains our results obtained for ε and Γ with models F and SC for Σ^- atoms for which experimental data exist. For the ΣA conversion cross section σ two expressions, (6) and (7), have been applied. Results obtained with expression(6), presented in II, are included into Table III for comparison with the new results obtained with expression (7). For the 23 data points, we get the following values for $\chi^2_{F(SC)}$ for our results obtained with model F (and SC):

$$\chi^2_F = \begin{cases} 38.1 \\ 19.5 \end{cases} \quad \chi^2_{SC} = \begin{cases} 55.0 \\ 33.3 \end{cases} \quad \text{for } \sigma \text{ expression } \begin{cases} (6), \\ (7). \end{cases} \quad (8)$$

We conclude that we get the best agreement with the data, when we apply model F. As discussed in I and II model F has the property that it leads to V_{NM} which is attractive at low densities encountered at the nuclear surface and repulsive at nucleon densities encountered inside nuclei. This means — in our local density approximation — that V is repulsive inside the nucleus, and has an attractive pocket at the nuclear surface (see Fig. 1).

TABLE III

Energy shifts $\varepsilon/\varepsilon^u$ and widths Γ/Γ^u of the lower/upper level of the indicated Σ^- atoms, calculated with models F and SC of the ΣN interaction. All energies are in eV.

Nucl.	Model	ε^a	ε^b	Γ^a	Γ^b	$\varepsilon^{u a}$	$\varepsilon^{u b}$	$\Gamma^{u a}$	$\Gamma^{u b}$
^{12}C	F	8.19	8.60	22.2	16.1	0.007	0.007	0.011	0.007
	SC	6.79	7.26	24.8	18.7	0.004	0.004	0.011	0.007
^{16}O	F	50.0	54.0	194.2	147.0	0.11	0.11	0.20	0.14
	SC	63.0	67.9	245.2	196.3	0.066	0.068	0.21	0.15
^{24}Mg	F	32.6	33.8	50.4	31.7	0.085	0.086	0.10	0.06
	SC	10.2	11.0	47.4	30.3	0.021	0.022	0.096	0.054
^{27}Al	F	67.3	70.1	113.2	73.2	0.22	0.23	0.28	0.16
	SC	24.4	27.2	109.4	72.4	0.064	0.067	0.27	0.15
^{28}Si	F	139.9	147.1	242.8	160.3	0.55	0.56	0.70	0.53
	SC	43.6	50.2	226.0	152.1	0.14	0.15	0.66	0.39
^{32}S	F	433.8	466.0	873.2	605.7	2.49	2.55	3.43	2.12
	SC	137.5	167.0	814.4	579.2	0.67	0.72	3.19	1.97
^{40}Ca	F	27.0	27.9	42.0	27.7	0.12	0.12	0.15	0.087
	SC	7.5	8.4	39.0	26.0	0.028	0.029	0.14	0.082
^{48}Ti	F	44.9	46.9	104.0	74.2	0.30	0.30	0.48	0.31
	SC	61.1	63.6	117.3	86.1	0.39	0.39	0.50	0.33
^{138}Ba	F	32.6	33.2	73.9	51.7	0.92	0.92	1.34	0.85
	SC	92.3	93.4	91.2	65.4	1.85	1.86	1.51	0.95
^{184}W	F	126.7	129.3	180.5	127.5	3.75	3.78	4.24	2.78
	SC	87.6	90.6	190.4	137.2	2.23	2.36	4.29	2.84
^{208}Pb	F	457.4	469.1	773.4	582.1	18.9	19.2	23.8	16.7
	SC	380.0	396.0	877.4	672.3	12.6	12.9	24.7	17.3

^a Expression (6) was applied for σ .

^b Expression (7) was applied for σ .

This conclusion of our analysis of Σ^- atoms agrees with the result of the phenomenological analysis of Σ^- atoms of Batty, Friedman, and Gal [19], and also with the analysis [20,21] of the pion spectra observed in Brookhaven in the strangeness exchange reaction on ^9Be target [22]².

The two parametrizations of σ are possible and lead to different results for ε and Γ , because the experimental points to which both of them are adjusted have big error bars, and they start at $p_\Sigma = \hbar k_\Sigma = 110 \text{ MeV}/c$, *i.e.*,

² There is one argument more in favor of model F: when applied to the Λ + nuclear matter system it leads to the semiempirical value of the Λ binding energy, *i.e.*, it solves the so called Λ overbinding problem [23].

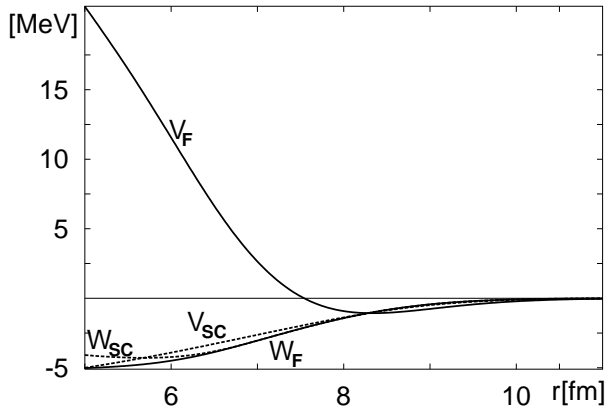


Fig. 1. Potentials V and W in ^{208}Pb obtained with model F and SC of the Nijmegen interaction. The potentials W were obtained with parametrization (6) of σ .

above the average Σ momenta in Σ^- atoms. As we see from Eq. (8), our results obtained with parametrization (7) reproduce the data points better than those obtained with parametrization (6). No doubt, a more precise measurement of the $\Sigma\Lambda$ conversion cross section at low energies would be most desired for discussing ε and Γ .

Now let us discuss other aspects of our results. We shall consider as a representative example the case the $n = 9$ state in Pb with parametrization (6) of σ . The real and absorptive potentials V and W of Σ^- in Pb are shown in Fig. 1. Here, W has been calculated with $\bar{k}_\Sigma = 0.40 \text{ fm}^{-1}$, the average Σ^- momentum in the lower ($n = 9$) state (if we used the average momentum in the upper ($n = 10$) state, the resulting curve could hardly be distinguished from the W curve in Fig. 1). Models F and SC of the Nijmegen interaction were used to obtain the results shown in Fig. 1. To distinguish them we use the subscripts F and SC.

The Bohr radius of the $n = 9$ orbit in Pb is 22.4 fm, whereas the r.m.s. radius of the charge distribution, $\langle r^2 \rangle^{1/2} \simeq 5.5 \text{ fm}$. Consequently, the finite size of the nuclear charge distribution is expected to have a negligible effects on the energy shift ε and the width Γ of the level, which indeed turn out to be about 0.2 % (for model F). Hence, one could safely neglect the effect of finite size of the nuclear charge distribution, as it was done in I. Also in the following discussion, we ignore this finite size effect.

Let us consider the problem whether perturbative treatment of the nuclear interaction in Σ^- atoms is justified. General arguments in favor of the perturbative treatment were discussed in I. Here, we consider the convergence of the perturbation expansion in the case of the lower state in Pb. Namely, we investigate how accurate is the first order of this expansion. The

pure Coulomb energy of the $n = 9$ state in Pb, $E_C = -2.6$ MeV, is changed by the strong interaction (model F) by the amount $\Delta\mathcal{E}_F = -\varepsilon_F + i\Gamma_F/2 = (-0.00046 + i0.00039)$ MeV. We see that the change in the real part of the energy, $-\varepsilon_F$, is extremely small compared to E_C , and we may expect the first order approximation $\varepsilon_{1F} = \langle\psi|V_F|\psi\rangle$ to be very close to ε (here ψ is the hydrogen-like function). Indeed, we find that in the $n = 9$ state in Pb model F leads to $\varepsilon_{1F} = 457.0$ eV, whereas $\varepsilon_F = 457.4$ eV. A comparison of our present results with the results of I shows that the situation with other Σ^- atoms is similar. There are two factors, V_F and W_F , which determine ε_F . In the region essential for the Σ^- atom, the real potential V_F has an attractive pocket, and the Σ wave function is pulled into this region. This accumulation of the wave function is counteracted by the absorptive potential W_F which diminishes the wave function in this region and thus acts similarly as repulsion. Thus the Σ wave function is not so much changed in this region by the combined action of V_F and W_F , and consequently ε_{1F} is close to ε_F . This may be illustrated in the case of the $n = 9$ state in Pb. If we consider only real V_F , *i.e.*, if we put $W = 0$, we get $\varepsilon_F[W = 0] = 494.3$ eV. This is greater than $\varepsilon_{1F} = 457.0$ eV which — in agreement with the variational principle — is a lower bound for $\varepsilon_F[W = 0]$. After switching on the absorptive potential W_F , we decrease ε_F to the value of 457.4 eV very close to ε_{1F} .

No doubt, the striking agreement of our results for ε_F with the first order perturbation results ε_{1F} is partly accidental. In case of model SC, we have: $\varepsilon_{SC} = 380.0$ eV, $\varepsilon_{SC}[W = 0] = 438.9$ eV, and $\varepsilon_{1SC} = 397.1$ eV. Here, the agreement — although reasonable — is less striking. The reason appears to be the pure attractive character of V_{SC} — the “repulsive” effect is produced entirely by W_{SC} ³.

The situation with the imaginary part of the energy is different. Here the entire imaginary part is due to W , and we do not expect the first order perturbation approximation, $\Gamma_1 = -2\langle\psi|W|\psi\rangle$, to be very accurate. For the $n = 9$ level in Pb, we get $\Gamma_{1F} = 716.6$ eV, whereas $\Gamma_F = 773.4$ eV, and here the accuracy of first order approximation is about 7%. In case of SC model, we have: $\Gamma_{1SC} = 715.2$ eV, $\Gamma_{SC} = 877.4$ eV, and here the accuracy is about 18%, *i.e.*, is worse.

In I, we used model F and approximated Γ by $\Gamma_{\bar{\rho}}$, the width of Σ in nuclear matter with density equal to the average density in the Σ^- atom, $\bar{\rho} = \langle\psi|\rho|\psi\rangle$, with the result $\Gamma_{\bar{\rho}} = 903.3$ eV. Thus the approximation applied in I turns out to be worse than the first order approximation Γ_1 .

³ Our estimate of the error in ε_1 presented in I appears to be not correct because our nonrelativistic ε_1 was compared with relativistic value of ε (determined in [19] from Klein-Gordon equation).

Now let us discuss another aspect of the theory of Σ^- atoms, namely the possibility of getting information on the nucleon distributions $\rho_p(r)$ and $\rho_n(r)$. To explore this possibility, we investigate the sensitivity of the calculated energy shifts ε and widths Γ to the applied forms of $\rho_p(r)$ and $\rho_n(r)$.

As an example, let us consider the properties of the Σ^- states in Ba⁴ calculated with model F of the Nijmegen interaction and with parametrization (6) of σ . For comparison with our results obtained with the ISM densities, we consider a 2-parameter Fermi (2pF) form $\rho(r) = \rho_0[1 + \exp((r - R)/a)]^{-1}$ for both point proton and neutron distributions.

As our 2pF model of the two densities ρ_p and ρ_n , we consider the model applied in [19]. The parameters R_p and a_p of $\rho_p(r)$ were adjusted — after folding with a Gaussian proton charge distribution — to the tabulated charge distribution [24]. For the much harder to determine neutron density, it was assumed that $a_n = a_p$ and $R_n = R_p + 0.25$ fm in a qualitative agreement with Hartree–Fock calculations. The parameters of the 2pF model are shown in Table IV, together with the mean square radii of ρ_p and ρ_n .

TABLE IV

Properties of Σ states in Ba calculated with different models of nucleon densities. Model F of the ΣN interaction, and parametrization (6) of σ were applied. All energies are in eV, and lengths in fm.

Model	R_p	$a_{p,n}$	R_n	$\langle r^2 \rangle_p^{1/2}$	$\langle r^2 \rangle_n^{1/2}$	ε	Γ	ε^u	Γ^u
ISM				4.80	5.41	32.6	73.9	0.92	1.34
2pF	5.80	0.433	6.05	4.77	4.96	6.84	22.0	0.17	0.29

Our results for the energy shifts and widths for the lower ($n = 8$) and upper ($n = 9$) levels in Ba, obtained with nucleon density model 2pF, and also ISM, are shown in Table IV. We see that when we switch from the ISM to the 2pF densities, we essentially decrease the resulting energy shifts and widths. The reason for it is that the ISM densities have longer tails than the 2pF densities.

We illustrate it in Fig. 2 in case of $W(r)$, and Γ obtained for the $n = 8$ level in Ba with the ISM and 2pF densities. As we see from Eqs. (2), (5), $W(r)$ depends predominantly on the proton density $\rho_p(r)$ (the dependence on $\rho_n(r)$ is only indirect through the exclusion principle operator Q). As we see in Fig. 2, $\rho_p(r)_{\text{ISM}}$ has a much longer tail than $\rho_p(r)_{\text{2pF}}$ — we have $\rho_p(r)_{\text{ISM}} > \rho_p(r)_{\text{2pF}}$ for $r \geq 6.4$ fm. Consequently, as is

⁴ In Ba we use the ISM results for both ρ_p and ρ_n , whereas in Pb (and W) the ISM results are available only for ρ_p .

seen in Fig. 2, $W(r)_{\text{ISM}}$ has a much longer tail than $W(r)_{\text{2pF}}$ — we have $W(r)_{\text{ISM}} < W(r)_{\text{2pF}}$ for $r \geq 6.4$ fm. Now, in Σ^- atoms just this tail region is important. Namely the Σ^- wave function Ψ at small distances behaves like r^{n-1} , and its square multiplied by $-W(r)$ attains its maximum in the tail region. If we approximate Ψ by the hydrogen-like function $\psi(\mathbf{r}) = R(r)r^{-1}Y_{l=n-1m}(\hat{r})$, then the product $-R(r)^2W(r)$ measures the contribution of the region around r to $\Gamma/2$ (when integrated this product over r , we get $\Gamma_1/2$, the first order approximation of $\Gamma/2$). The product $-R^2W$ is shown in Fig. 2, and obviously this product for the ISM densities is much bigger and is shifted towards larger distances. The explanation why the ISM densities lead to larger energy shifts than the 2pF densities is similar.

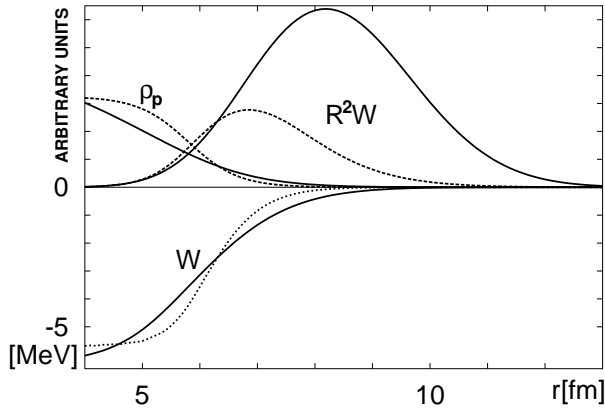


Fig. 2. Proton density ρ_p , the imaginary potential W , and the product $-R^2W$ in the $n = 8$ state in Ba, obtained with the ISM (solid curves) and 2pF (broken curves) densities. Model F and parametrization (6) of σ were applied.

Let us notice that the product $-R^2W$ (and similarly the product $-R^2V$) attains its maximum in the tail of the density distributions, especially for ISM, where both the densities and their gradients are small. This means that the YNG effective interaction applied in our work may be less burdened by the ambiguities in the choice of the intermediate state energies in the reaction matrix equation, because this choice is less important at low densities. Furthermore, the smallness of the density gradients certainly improves the accuracy of the local density approximation.

The authors express their gratitude to Prof. Sławomir Wycech for his illuminating comments. This research was partly supported by the Polish State Committee for Scientific Research (KBN) under grant no. 2P03B7522.

REFERENCES

- [1] G. Backenstoss, T. Bunacin, J. Egger, H. Koch, A. Schwitter, L. Tauscher, *Z. Phys.* **A273**, 137 (1975).
- [2] C.J. Batty, S.F. Biagi, M. Blecher, S.D. Hoath, R.A.J. Riddle, B.L. Roberts, J.D. Davies, G.J. Pyle, G.T.A. Squier, D.M. Asbury, *Phys. Lett.* **74B**, 27 (1978).
- [3] R.J. Powers *et al.*, *Phys. Rev.* **C47**, 1263 (1993).
- [4] J. Dąbrowski, J. Rożynek, G.S. Anagnostatos, *Acta Phys. Pol.* **B32**, 2179 (2001).
- [5] J. Dąbrowski, J. Rożynek, G.S. Anagnostatos, *Europ. Phys. J. A* in press.
- [6] N.M. Nagels, T.A. Rijken, J.J. de Swart, *Phys. Rev.* **D12**, 744 (1975); **15**, 2547 (1977).
- [7] N.M. Nagels, T.A. Rijken, J.J. de Swart, *Phys. Rev.* **D20**, 1663 (1979).
- [8] P.M.M. Maessen, T.A. Rijken, J.J. de Swart, *Phys. Rev.* **C40**, 2226 (1989); *Nucl. Phys.* **A547**, 245c (1992).
- [9] T.A. Rijken, V.G.J. Stoks, Y. Yamamoto, *Phys. Rev.* **C59**, 21 (1999).
- [10] Y. Yamamoto, T. Motoba, H. Himeno, K. Ikeda, S. Nagata, *Progr. Theor. Phys. Suppl.* **117**, 361 (1994).
- [11] J. Dąbrowski, J. Rożynek, *Phys. Rev.* **C23**, 1706 (1981).
- [12] J. Dąbrowski, J. Rożynek, *Acta Phys. Pol.* **B14**, 439 (1983).
- [13] A. Gal, G. Toker, Y. Alexander, *Ann. Phys.* **137**, 341 (1981).
- [14] E. Oset, L.L. Salcedo, R. Brockmann, *Phys. Rep.* **188**, 79 (1990).
- [15] G.S. Anagnostatos, *Canad. J. Phys.* **70**, 361 (1992).
- [16] G. S. Anagnostatos, *Int. J. Theor. Phys.* **24**, 579 (1985).
- [17] G.S. Anagnostatos, P. Ginis, J. Giapitzakis, *Phys. Rev.* **C58**, 3305 (1998).
- [18] G.S. Anagnostatos, *Int. J. Mod. Phys.* **E5**, 557 (1996).
- [19] C.J. Batty, E. Friedman, A. Gal, *Phys. Rep.* **287**, 385 (1997).
- [20] J. Dąbrowski, J. Rożynek, *Acta Phys. Pol.* **B29**, 2147 (1998).
- [21] Y. Shimizu, Ph.D. thesis, University of Tokyo, 1996 (unpublished).
- [22] S. Bart *et al.*, *Phys. Rev. Lett.* **83**, 5238 (1999).
- [23] J. Rożynek, J. Dąbrowski, *Phys. Rev.* **C20**, 1612 (1979).
- [24] H. de Vries *et al.*, *At. Data Nucl. Data Tables* **36**, 495 (1987).